



# Investigation on thermal ageing impact on dielectric properties of natural ester oil

Soumya Thakur<sup>1</sup> · R. Sarathi<sup>1</sup> · M. G. Danikas<sup>2</sup>

Received: 23 April 2019 / Accepted: 26 September 2019 / Published online: 1 October 2019  
© Springer-Verlag GmbH Germany, part of Springer Nature 2019

## Abstract

Ester oils are evolving as next-generation transformer insulants, and it is essential to understand their characteristic variation upon thermal ageing. Corona inception voltage reduces with thermally aged ester oil under AC and DC voltages. The UHF signal generated due to corona discharge activity has energy content in the range 0.4–4 GHz. The magnitude and energy content of the UHF signal formed due to corona activity increases with thermally aged oil. Ionic mobility studies are carried out to understand the impact of thermal ageing on polarization and depolarization current, ion concentration, and ionic radius formed in the oil. Thermal ageing of ester oil leads to an increase in the ionic mobility of oil samples along with an increment in the ionic concentration. The conductivity of oil is observed to increase with ageing, accompanied by a reduction in ionic radii. The effect of voltage stress shows enhanced conductivity for thermally aged oil samples. Dielectric response spectroscopy exhibits higher loss and permittivity values for thermally aged oils. The physicochemical analysis shows a gain in viscosity, moisture content and turbidity, and a marginal loss in thermal conductivity due to the formation of new molecular species. UV analysis exhibits a significant redshift in the oil sample aged at a higher temperature.

**Keywords** Natural ester oil · Thermal ageing · Corona inception voltage · Ionic mobility · Dielectric response spectroscopy

## 1 Introduction

Ester oils are now gaining considerable importance, being used as insulants in transformers. They are considered as next-generation transformer insulation owing to their superior thermal properties, higher flash point, fire point and high breakdown strength. They have a low potential for corrosive sulphur and moisture ingress properties and are readily biodegradable [1]. For higher sustainability and economic stability, it is essential to ensure proper uninterrupted operation of the transformer. The oil in a transformer acts as an information source containing up to 70% diagnostic data [2]. The researchers over the world are trying to understand the adoption of fault diagnosis techniques and interpretations carried out for transformer oil applicable for ester oil [3]. Regular condition monitoring and analysis of

various physicochemical changes in oil, during transformer operation, can help us to mitigate the possible failure of the transformer.

Thermal stress is reported to adversely affect the electrical properties of the oil, leading to a compromise in its role as an insulant as well as a coolant [4]. Hotspot formation and overload or fault conditions can significantly increase the transformer oil temperature to 200 °C [5]. Recently, Park and Han have indicated that hot spot temperature is much higher with ester oil compared to mineral oil. They have analysed the thermal characteristics of oil adopting computational fluid mechanics for distribution and power transformer fluids and have indicated that for natural ester oil, average hot spot temperature is 24% higher than the mineral oil. This increment is due to higher kinematic viscosity of ester oil, which restricts the fluid motion reducing its cooling efficiency [6]. Hot spot temperature directly impacts the transformer loading capability and the acceleration of the degradation process of oil insulation [7]. Bandara et al. [8] have studied the impact of thermal ageing of oil to quantify changes in dielectric loss and the colour index of oil.

One of the causes for failure of liquid insulation is corona discharge, which occurs due to the intensification of

✉ R. Sarathi  
rsarathi@iitm.ac.in

<sup>1</sup> Department of Electrical Engineering, Indian Institute of Technology Madras, Chennai 600 036, India

<sup>2</sup> Department of Electrical and Computer Science Engineering, Democritus University of Thrace, 67100 Xanthi, Greece

the electric field at the weak links or due to protrusions in the winding and at the edges inside the transformer. These corona discharges radiate electromagnetic waves in ultra-high frequency (UHF) range. UHF sensing technique is gaining popularity as it is a non-invasive, non-destructive, highly sensitive method with a high signal-to-noise ratio. Online condition monitoring using UHF sensor enables one to determine the occurrence of such incipient discharges in transformer insulation [9].

A detailed review of results obtained from various condition monitoring and diagnostic techniques suggests that most transformer failures are attributed to winding and insulation failure. These are accompanied by increased partial discharge, contact resistance and problems with the cooling system, which increases operating temperature [10]. A significant number of transformer failures have evoked renewed interest in understanding the impact on dielectric properties due to variation in conduction mechanism [11]. Effect of accelerated thermal ageing of oil is reflected in its dielectric properties especially with the variation in dissipation factor, dielectric constant and ionic mobility.

Thermal ageing affects the dielectric properties of the insulating liquid. These changes are reflected in polarization and depolarization current characteristics, which can be effectively correlated by dielectric response spectroscopy (DRS) analysis. Bandara et al. [8] have reported that though the relaxation time is unaffected by the ageing process, polarization and conduction mechanism were observed to be greatly enhanced by the ageing by-products. Bartnikas has concluded that dielectric losses in liquids occur due to the space charge polarization, dipole orientation and ionic conduction. These losses are temperature and viscosity dependent and are observed to increase with an increase in the aromatic content of oil [12]. Wang et al. [13] analysed the frequency-domain spectroscopy for pressboard sample and determined that deterioration due to thermal ageing can lead to an increment in the conductivity of the insulation. Similar results on the understanding of ionic conductivity and dielectric response of thermally aged ester oil are scanty.

Ionic mobility of a liquid can be defined as the magnitude of charge transferred through the bulk of the insulation. It greatly influences the space charge dynamics and the electric field associated in the medium. As the medium and physico-chemical state of liquid affects the type of charge carriers and thus the ionic mobility is a material-specific property. Yang et al. [14] have discussed the different methods applicable for the measurement of ionic mobility along with their advantages and disadvantages. Lv et al. [15] have given an interesting insight into the impact of the presence of nano-sized impurities in oil over the conduction properties and ionic mobility of liquid dielectrics. Variation of ionic mobility with temperature shows a direct relationship indicating that the ionic drift is a thermally activated phenomenon [16].

Having known all these aspects into consideration, methodical experimental studies were carried out to understand the impact of thermal ageing of natural ester oil, at different temperatures on (1) variation due to thermal ageing on corona inception voltage and the characteristics of UHF signals generated, (2) ionic mobility analysis for aged oil sample to understand the impact of ageing on ionic conductivity, concentration and effective ionic radii, (3) dielectric response analysis of thermally aged oil, and (4) analysis of the characteristic variation with thermally aged oil through UV–Vis spectra analysis, FTIR spectra, viscosity, turbidity, thermal conductivity and moisture content of oil as a consequence of ageing.

## 2 Experimental set-ups

### 2.1 Thermal ageing

The present analysis is carried out on rapeseed natural ester oil procured from M&I materials (MIDEL 1204). In order to simulate the effect of thermal degradation in oil insulation of a transformer in laboratory conditions within a short span of time, accelerated ageing of oil was carried out. The pressboard used was commercially procured from Andrew Yule Pvt. Ltd. The pressboard samples of 4 cm × 4 cm × 2 mm dimensions were heated at 120 °C for 4 h to remove any possible moisture and then kept immersed in oil for 6 h at 70 °C to ensure proper impregnation. One litre of rapeseed natural ester oil, oil-impregnated pressboard and copper were kept in a temperature-controlled reaction vessel, in which a nitrogen atmosphere was maintained by constant purging with nitrogen at a regulated pressure. The weight ratio of oil/pressboard/copper was maintained as 10:1:1.

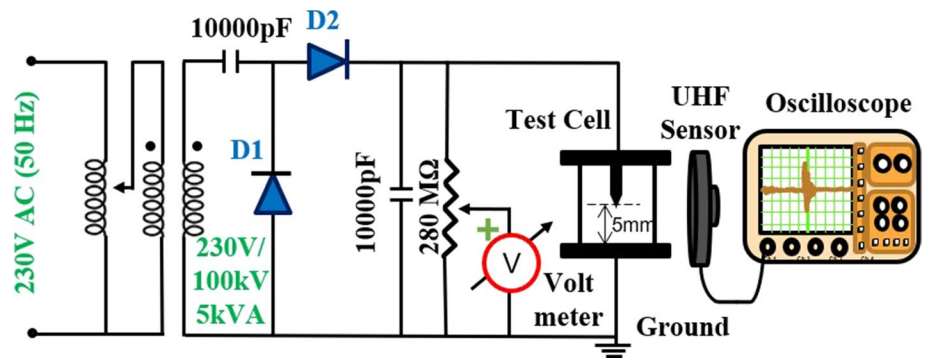
IEEE guide C57.147 for acceptance and maintenance of natural ester fluids restricts the upper limit for thermal ageing studies at 180 °C, to avoid fluid scorching such that the watt density does not exceed 2 W cm<sup>-2</sup> (12 W in<sup>-2</sup>) [17]. Thus, in the present analysis, thermal ageing was carried out at 70 °C, 140 °C and 180 °C for a duration of 500 h after which the oil was taken out and kept in a desiccator to minimize the influence of moisture.

The analysis was done on fresh oil referred to as virgin oil and thermally aged oil, aged at 70 °C, 140 °C and 180 °C for 500 h referred as Sample A, Sample B and Sample C, respectively.

### 2.2 Experimental set-up for corona inception voltage studies

Figure 1 shows the experimental set-up used for measuring corona inception voltage. The experimental set-up can be classified into three important sections: high-voltage source

**Fig. 1** Experimental set-up for corona inception and breakdown studies



with measuring unit, the test cell and the UHF sensor along with high-bandwidth oscilloscope.

High AC voltage was generated by using a test transformer (100 kV, 5 kVA, 50 Hz) and directly connected to the test cell. The transformer output connected to voltage-doubler circuit, for DC voltage generation. The AC and DC voltages were measured using capacitance and resistance divider, respectively.

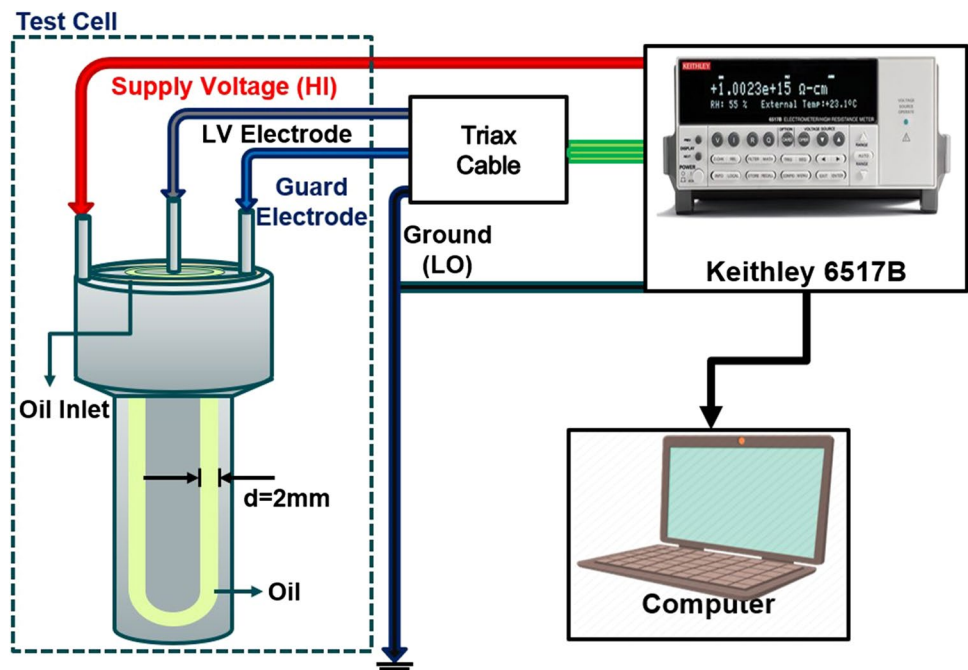
Needle plane configuration was used for corona inception studies. The top high-voltage needle electrode used was with a 50- $\mu\text{m}$  radius of curvature. The bottom ground electrode flat ground electrode of 5 cm diameter was kept at a constant gap of 5 mm from the needle electrode. For capturing electromagnetic signals generated on the inception of corona activity in oil samples, a broadband type UHF sensor was used. The UHF sensor was connected to a Lecroy Model Wavepro high-frequency digital storage oscilloscope (3.5 GHz bandwidth, sampling rate 40 GSa/s). Cable

impedance of 50  $\Omega$  was matched with the input impedance of oscilloscope. A constant gap of 20 cm was maintained between the UHF sensor and the test cell.

### 2.3 Experimental set-up for ionic mobility and dielectric analysis

Figure 2 shows the experimental set-up for measuring the ionic mobility of different oil samples. Keithley 6517B is used for supplying voltage and measuring current. A triax cable is connected to the measuring (LV) electrode, guard electrode of test cell and ground, which is connected to the ground of the instrument. The stainless-steel test cell with Teflon insulation is configured as a cylindrical capacitor. The guard ring acts as a shield for measurement. The test cell capacitance is  $55 \pm 5\%$  pF, test cell liquid volume is 50 mL, and maximum operating temperature is 150  $^{\circ}\text{C}$ . Keithley electrometer is interfaced with a computer using LabVIEW

**Fig. 2** Experimental set-up for ionic mobility study



platform. For the current analysis, conductivity of a different oil was tested at a different voltage magnitude following reverse polarity method. Each measurement was carried out for 4 cycles, 500 s each. The first cycle data were discarded as they are influenced by stray charges. The ionic mobility measurements were taken at a controlled temperature of 30 °C.

Dielectric response study was performed following IEC 60247 [18]. Test cell used for ionic mobility study is used for dielectric response study. Omicron dielectric response analyser was used for the study along with temperature-controlled thermostat. The temperature range was varied from 30 to 90 °C. The supply frequency was varied from 0.1 Hz to 1 kHz.

## 2.4 Physicochemical studies

UV–Vis analysis of oil was carried out using Agilent Cary 3500 UV–Vis spectrophotometer, with a scan rate of 1000 nm s<sup>-1</sup>. One-millimetre-path length cuvettes were employed for the measurement with hexane as the baseline correction solvent, to avoid errors in spectral measurements. FTIR analysis was carried out using Jasco IR spectrometer (FTIR-4100) by operating it in the range 400–4000 cm<sup>-1</sup>. For baseline correction, sodium chloride disc pellets were chosen.

Viscosity measurement of the oil samples carried out using Anton Parr Physica MCR 301 microviscometer. Turbidity of oil samples was measured using 2100Q portable turbidity meter. Thermal conductivity values were obtained using Hot disc thermal analyser TPS 500. Moisture content measurements were carried out with the help of 899 Coulometer Karl-Fischer titrator.

## 3 Results and discussion

### 3.1 Corona inception voltage analysis

Figure 3 shows the variation in corona inception voltage (CIV) of a virgin as well as thermally aged ester oil samples. The values are the average value of 25 readings. The deviation in data is observed less than 3%, and hence, the deviation is not indicated. The CIV is high under negative DC followed with positive DC and AC voltages. It is observed that compared to negative polarity, the inception of corona occurs at lower voltage under positive polarity. This could be attributed to the generation of aiding electric field at the tip of the electrode in case of positive polarity. Azcarraga et al. [19] have indicated that the ionization of the liquid is faster under positive polarity compared to negative polarity. Xiang et al. have compared the effect of polarity on the typical current signal generated during the

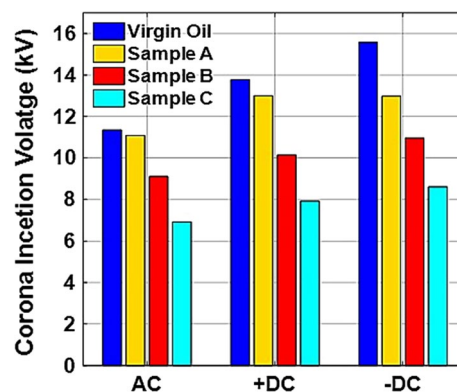


Fig. 3 Corona inception voltage under AC, + DC and – DC voltage for different oil sample

inception of streamer in oil under DC stress. Intense light and continuous current component were observed to generate in case of positive polarity, whereas negative polarity was accompanied by single current pulse and light signal. Further, they have observed that ahead of positive point, positive space charges get accumulated which suppress streamer inception under positive polarity and weaken the near-tip field, whereas accumulation of positive space charges on the negative tip decreases the inception voltage under negative polarity as the near-tip field then gets enhanced [20]. This clearly indicates that the severity of discharges is high under positive DC voltage.

It is observed that the CIV reduces with thermally aged oil, under AC and DC voltages. The inception of corona activity and its propagation basically rely on local conditions which include the radius of curvature of the top needle electrode, size and shape of the contaminated particle [3]. Beroual et al. [21] have reported that streamer propagation in the liquid is influenced by multiple factors, predominantly electronic and gaseous phenomena, where positive streamers exhibit higher velocity. Devins et al. [22] have studied pre-breakdown phenomena in dielectric liquids and have reported that at elevated temperature streamers of higher velocity and longer length are formed. Thermal ageing of oil can lead to higher susceptibility of transient cavity formation which can attribute to a decreased inception voltage value.

Figure 4a shows a typical UHF signal formed due to corona activity in ester oil and its corresponding FFT is shown in Fig. 4b. The dominant frequency content is found to be around 1 GHz with its energy content high in the range 0.4–4 GHz. The characteristics of the UHF signal formed due to corona activity, with thermally aged oil is also the same as it is observed with virgin oil. Judd and Cleary [23] have proposed direct relation of signal energy to  $q^2$ . Figure 5 shows the variation of signal energy as a function of a peak-to-peak voltage magnitude of the UHF signal formed due to corona activity for 25 consecutive signals acquired due to

**Fig. 4** Typical **a** UHF signal and **b** its corresponding fast Fourier transform of UHF signal obtained for different oil sample

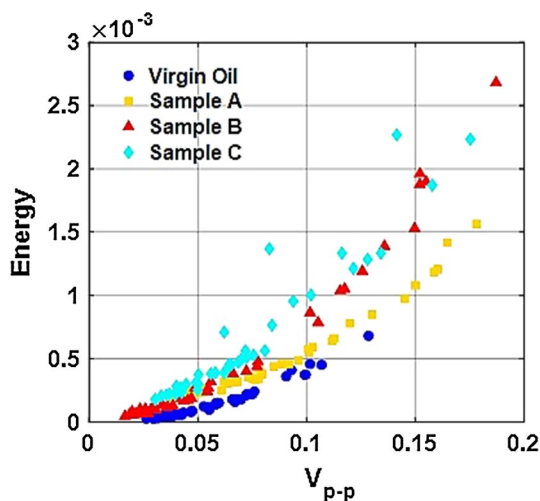
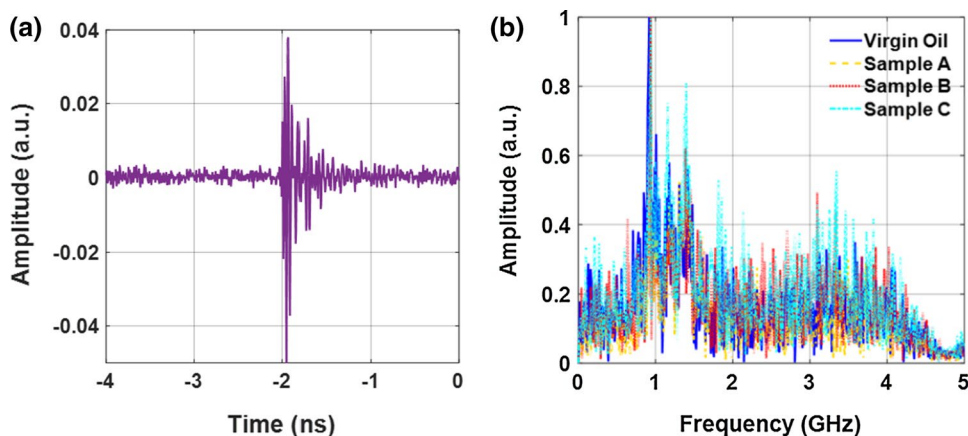


**Fig. 5** Energy–peak-to-peak voltage ( $V_{p-p}$ ) characteristics for different oil samples

corona activity. The energy content of the UHF signal can be calculated as

$$E_i = \frac{\sum_i A_i^2}{R_L} \tag{1}$$

where  $A_i$  is signal amplitude (a.u.) and  $R_L$  indicates the cable impedance which is 50  $\Omega$ . Figure 5 shows that ageing of oil samples at higher temperature leads to the occurrence of discharge of higher magnitude and correspondingly energy of corona discharges increases with ageing temperature.

### 3.2 Ionic mobility of thermally aged oil

The conductivity of a sample is greatly influenced by ionic mobility and concentration at a given applied electric field. In order to understand the impact of thermal degradation on

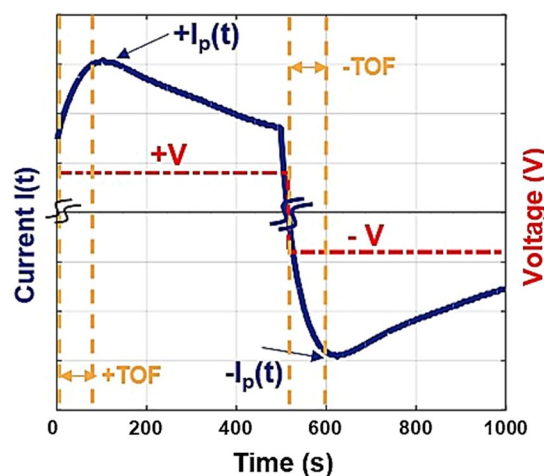


**Fig. 6** Typical current–time graph obtained for ionic mobility experiments for application of reverse polarity square wave voltage for rapeseed natural ester oil

conductivity, it is paramount to understand the changes in ionic mobility of aged samples.

Current across test set-up (Fig. 2) was measured by applying square wave voltages. Yang et al. have emphasized the importance of polarity reversal in ionic mobility measurements. Dual-polarity application shows negligible dependence on rest time between measurements and is thus superior and reliable [14]. The present analysis of polarity reversal was carried out after a time period of 500 s. Figure 6 shows a typical voltage applied and current waveform across the test cell. The current waveform is an illustration of an initial current rise which slowly decreases after a certain time period. The peak of current obtained is demonstrated as  $I_p$  and time required to reach the peak current is denoted as time of flight (TOF). Four consecutive cycles are recorded for each sample at different voltages. The initial voltage cycle applied acts as a driving force to bring out ions from the bulk of oil medium near the electrode from where they

are swept to the other electrode on the reversal of voltage polarity. Adamczewski and Januszajtis [24] have reported that ionic mobility is greatly influenced by field enhanced emission and physicochemical properties of oil. Thus the current graph obtained for different oil samples will have material-specific waveform.

Figure 7 shows the  $I_p$  and TOF values obtained for virgin and aged oil samples for negative and positive polarity application. The error bar indicated shows less than 5% deviation, denoting reliability of measurement. It is observed that an inverse relation is found between  $I_p$  and TOF. Effect of polarity shows a negligible impact on  $I_p$  values, whereas TOF values are high for negative polarity voltages for virgin oil. Thermal degradation shows an increase in conduction current and decreases in TOF for both polarities.

Polarity has a negligible effect on TOF values at a higher voltage and for thermally aged oil sample at higher temperatures. Charge transfer in liquids can occur due to charge injection, separation or motion of the double layer. The enhancement of charge transfer on the increase in applied voltage can be understood as the effect of electrohydrodynamic phenomena. It explains that increased conduction in the bulk dielectric is an effect of enhanced electric field influencing the drift of ions.

The ionic mobility of oil samples could be calculated using the time taken by these ions to reach the peak of conduction (TOF). The relation between ionic mobility  $\mu$  and TOF is [25],

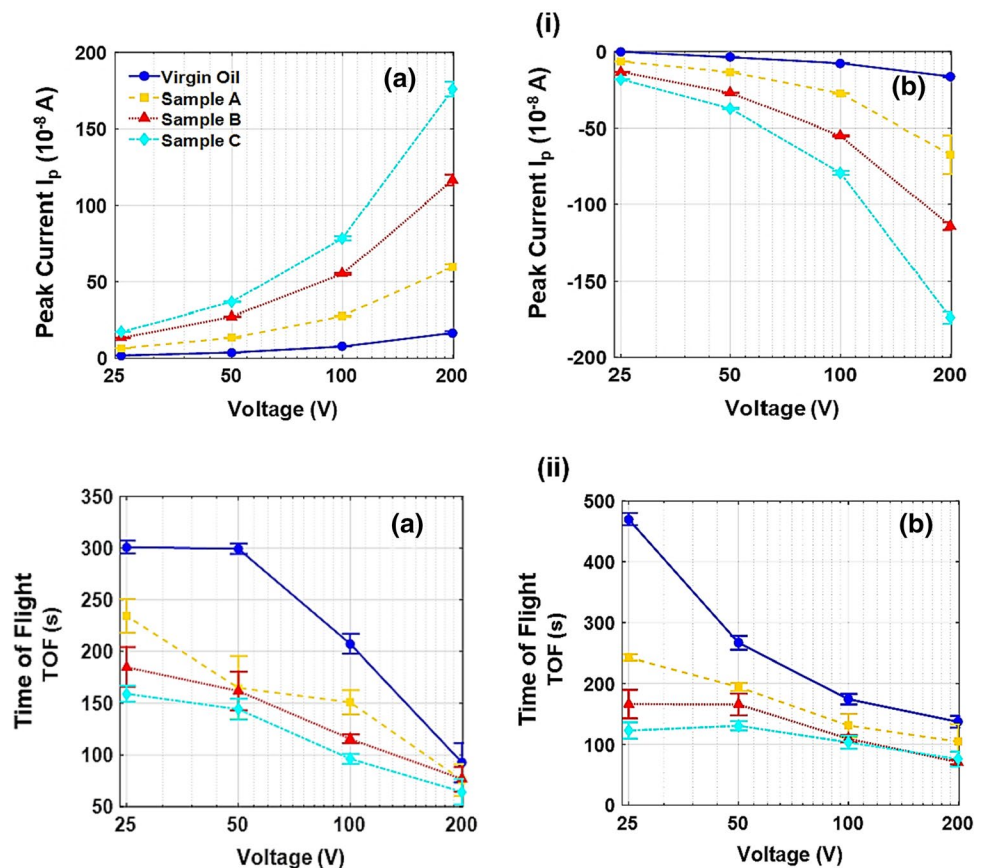
$$\mu = \frac{d^2}{V * TOF} \tag{2}$$

Figure 8 shows variation in ionic mobility of virgin and thermally aged ester oil under positive and negative polarity of the applied voltage of different magnitudes. For ester oil insulation, it was observed that an increase in voltage led to a decrease in ionic mobility. This can be explained as a result of a steep decrease in TOF value for higher voltage values. Thermal ageing at higher temperatures shows higher conductivity in both positive polarity and negative polarity. This could be attributed to changes occurring at the molecular level as a consequence of ageing at a higher temperature. Lv et al. [15] have reported a sudden decrease in ionic mobility as a consequence of an increase in the applied electric field.

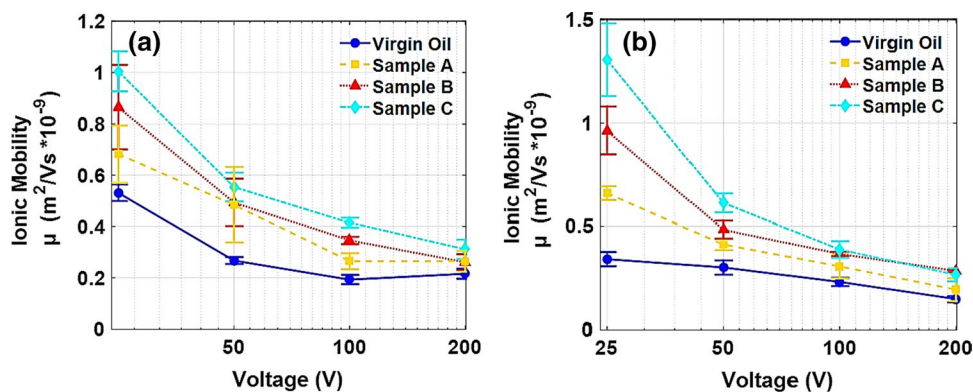
Conductivity in dielectrics can be understood by means of measuring initial short-pulse current analysis at low electric field stress as per IEC 61620. The ionic conductivity ( $\sigma$ ) can be determined as [26],

$$\sigma_o = \frac{I(t)\epsilon_o}{C_o V} \tag{3}$$

**Fig. 7** Effect of supply voltage and thermal ageing on **i** Peak current value and **ii** time of flight (TOF) for **a** positive polarity and **b** negative polarity voltage application



**Fig. 8** Effect of test voltage on ionic mobility for different oil samples aged at different temperatures for **a** positive polarity, **b** negative voltage application



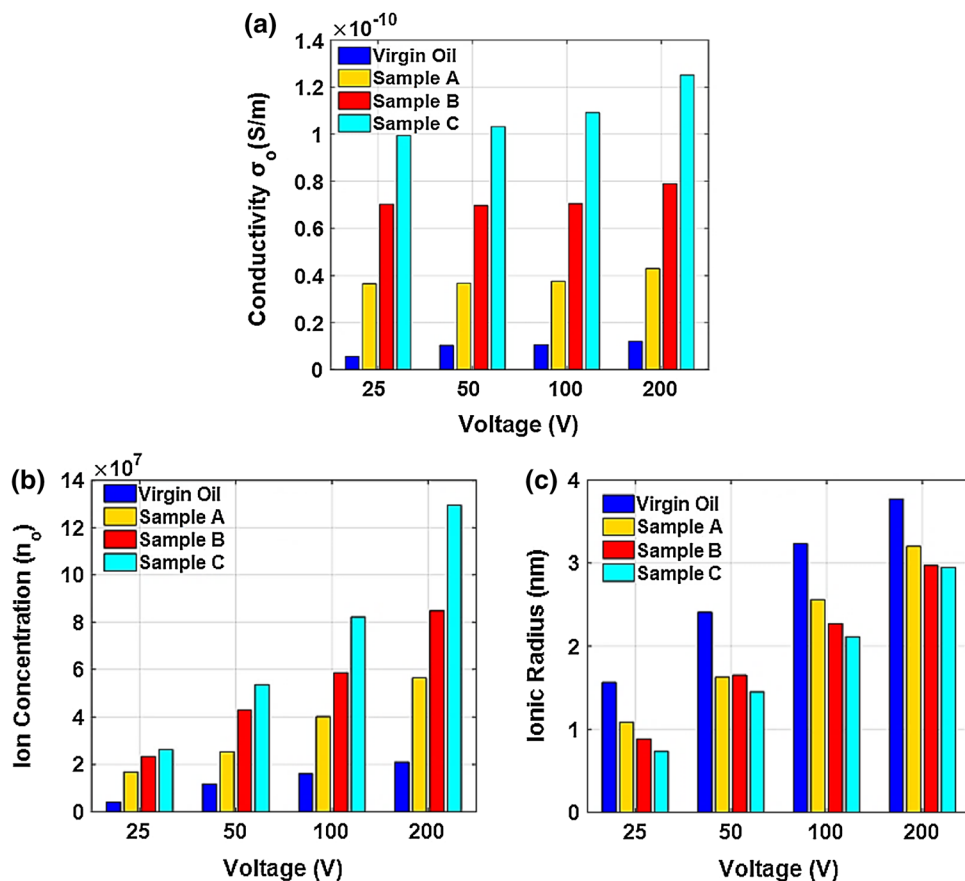
where the initial current  $I(t)$  measured at  $t=1$  is taken as the standard for determining the conductivity.  $\epsilon_o$  corresponds to the permittivity of free space,  $C_o$  is the test cell capacitance and  $V$  is the applied voltage. Yang et al. [14] have calculated the ionic conductivities of oil samples and indicated that it shows close correlation with conductivity measured by frequency-domain spectroscopy. The conductivity variation with the thermally aged oil is shown in Fig. 9a. It is observed that thermal ageing can cause enhanced conductivity of the liquid.

From the above analysis, the ionic concentration at equilibrium can be estimated. Onsager has proposed the possibility of calculation of chemical time lag, given that the molecular concentration and ionic concentration are comparable to the size of free ions and ion pairs. It was reported that the ionic concentration at low voltage is determined by dissociation and recombination of ions [27].

In the present analysis equilibrium, ionic concentration is calculated using the following equation,

$$n_{eq} = \frac{\sigma}{q(\mu^+ + \mu^-)} \tag{4}$$

**Fig. 9** Effect of test voltage and thermal ageing on **a** conductivity, **b** ionic concentration and **c** ionic radius for different oil samples



where  $n_{\text{eq}}$  denotes the ionic concentration at equilibrium,  $\sigma$  is the conductivity value,  $q$  denotes the fundamental electron charge and  $\mu^+$  and  $\mu^-$  refers to the ionic mobility determined for positive and negative voltage polarity.

Figure 9b shows the variation in ionic concentration for different oil samples. It is observed that with increase in ageing temperature, the number of ions generated in the oil increases exponentially at all the voltages. With an increase in applied voltage the ionic concentration increases which can be understood by electrohydrodynamic phenomena. These results support the enhancement of ionic conduction and peak current value. The increase in concentration gives insight into the degradation mechanism of oil upon exposure to thermal stress.

Thermal ageing leads to the breakdown of bulky hydrocarbons into oxygenated polar molecules. Due to thermal ageing, unsaturated fatty acids are converted to saturated fatty acids, i.e., total unsaturation decreases, the viscosity of oil increases, polar molecules are formed due to oxidation, polymerization and hydrolysis of oil [28]. These chemical changes affect the ionic radii of oil. The enhancement in the number of ionic concentration leads to an interesting observation on effective ionic radii. For calculating the effective ionic radii ( $R$ ) for a given oil sample, Walden's formula was employed, which describes the presence of an inverse relationship between ionic mobility and viscosity ( $\eta$ ) of the oil sample. This is also supported by Stoke's law, which defines this constant of inverse proportionality of viscosity and ionic mobility [29].

$$\mu\eta = \frac{q}{6\pi R} \quad (5)$$

here  $q$  corresponds to the fundamental charge of an electron. Viscosity ( $\eta$ ) of oil samples were measured (Table 1) and  $R$  was calculated using Eq. (5) as shown in Fig. 9c. The effect of applied voltage has a proportional effect on ionic radii. It is interesting to note that ionic radii decrease with thermal ageing. The contaminants/chemical structure variation of liquid due to thermal ageing causes variation in ionic conductivity and the ionic radii.

### 3.3 Dielectric response spectroscopy

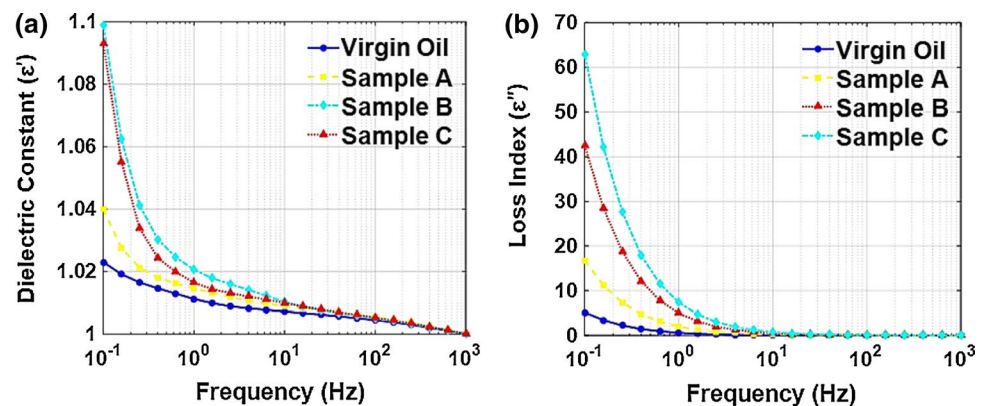
Figure 10 shows the real and imaginary permittivity of oil samples at 90 °C with frequency varying in 0.1–1000 Hz range. As indicated in Sect. 3.2, thermal ageing results in the formation of ions of smaller size and higher concentration, enhancing the ionic mobility, which could attribute in enhanced permittivity of oil. Wang et al. [13] have observed that ageing of oil leads to larger polarization and depolarization currents which results in increased permittivity especially in the lower frequency range.

At higher temperatures, ester oil undergoes oxidative degradation of unsaturated fatty acids. The free radical reaction of the hydrogen atom leads to enhanced conduction in the oil matrix. Singha et al. [30] have studied the impact of thermal ageing on the dielectric strength of ester

**Table 1** Variation in physicochemical parameters with ageing

| Property                    | Sample     |          |          |          |
|-----------------------------|------------|----------|----------|----------|
|                             | Virgin oil | Sample A | Sample B | Sample C |
| DDP (a.u.)                  | 6          | 23       | 97       | 197      |
| Viscosity (Pa s)            | 0.058      | 0.062    | 0.067    | 0.072    |
| Turbidity (NTU)             | 0.66       | 0.76     | 1.17     | 2.69     |
| Thermal conductivity (mW/K) | 0.16       | 0.15     | 0.12     | 0.11     |
| Moisture content (ppm)      | 67         | 234      | 356      | 412      |

**Fig. 10** Variation in complex permittivity of different oil samples at 90 °C **a** dielectric constant, **b** loss index





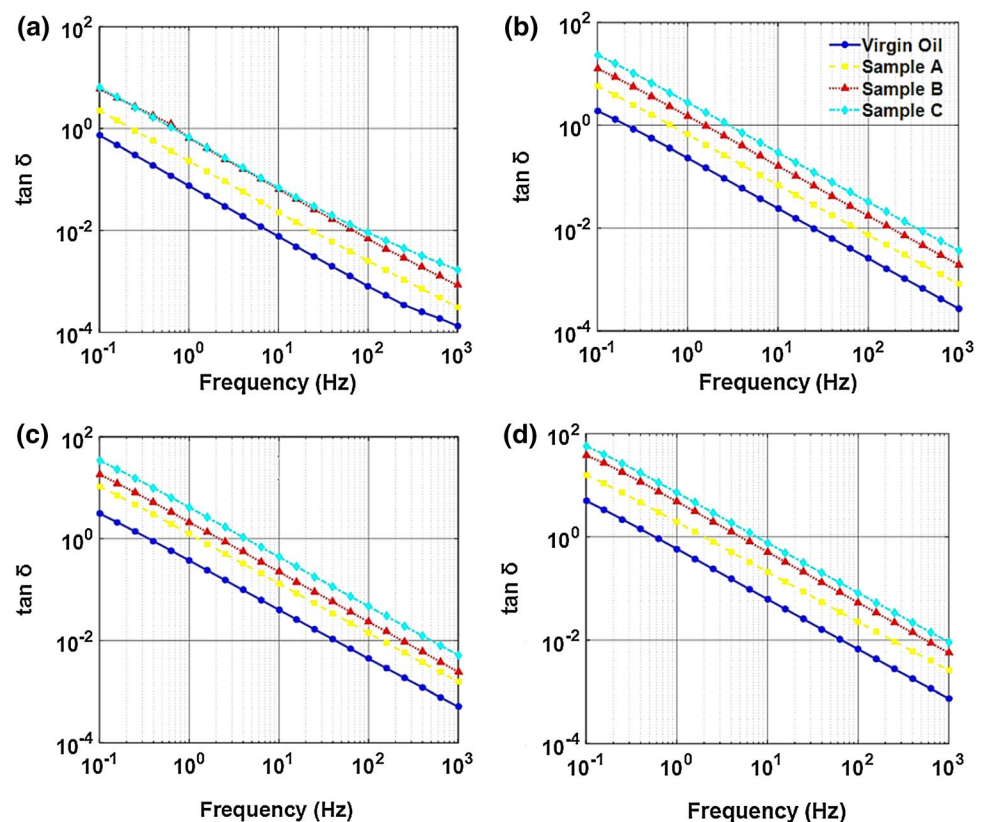
oil and have found that ageing leads to enhancement of acidity and power factor losses.

The increase in permittivity values due to ageing is also accompanied by an increase in dielectric losses in aged oil. Figure 11 shows variation in loss factor ( $\tan \delta$ ) of thermally aged oil samples at different temperatures. Thermal ageing at higher temperatures showed a higher loss factor. This characteristic is indicative of heat and dielectric losses occurring in the liquid dielectric due to the orientation of dipoles of polar molecules formed in oil as a consequence of thermal degradation. The frequency of response is varied from 0.1 Hz to 1 kHz. At lower frequency, losses are more prominent due to slow polarization–depolarization in bulk of liquid insulation. In liquid dielectrics, specific conduction is constant and loss tangent is inversely proportional to frequency [12]. Jonscher [31] has explained the enhanced dielectric response as a result of low-frequency dispersion (LFD), which can occur due to the hopping of charge carriers.

### 3.4 Physicochemical analysis

Thermal ageing causes characteristic changes in the properties of the material. The analysis was carried out through various methods.

**Fig. 11** Dielectric loss ( $\tan \delta$ ) of different oil samples at different measuring temperatures **a** 30 °C, **b** 50 °C, **c** 70 °C and **d** 90 °C



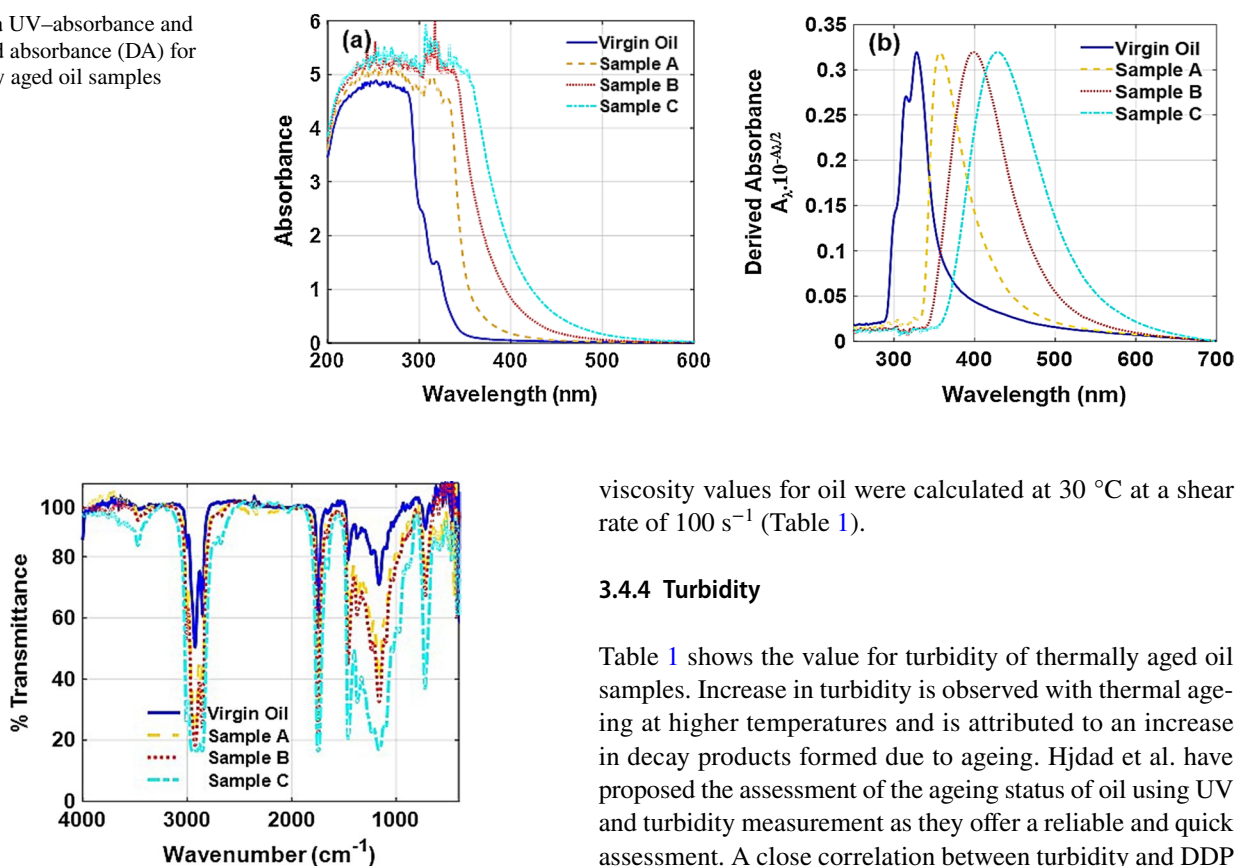
#### 3.4.1 UV–Vis absorbance

Figure 12a shows the variation in UV absorbance for the thermally aged specimen. A chromatic shift towards the red end is observed in aged oil samples which lead to pigmentation due to the oxidative reactions occurring in the oil at elevated temperatures. Saha et al. have analysed the UV–visible spectra for aged oil and reported the increase of colour index of aged oil is associated with an increase in absorbance of oil which corresponds to the presence of conjugated double bonds or aromatic compounds. The results indicate that the absorbance of oil builds up monotonically with ageing time at a much higher rate in the air than in nitrogen ambience [32]. The breakdown of ester linkage of triacylglycerols resulting in the production of di- and mono-acylglycerols, glycerol, and free fatty acids lead to change in colour and density of oil [28]. The progressive pigmentation in oil can be quantified using derived UV absorbance analysis. The derived absorbance (DA) is estimated using:

$$DA = A_{\lambda} 10^{-A_{\lambda}/2}. \quad (6)$$

Figure 12b shows a progressive redshift in the peak of DA indicating darkening of oil due to free radical and oxidative reactions. As per ASTM D6802, the area under the absorbance curve in 360–600 nm range gives the dissolved decay product (DDP) of the oil samples [33]. The DDP values

**Fig. 12** **a** UV-absorbance and **b** derived absorbance (DA) for thermally aged oil samples



**Fig. 13** FTIR spectra for virgin ester oil and oil samples aged at 70 °C, 140 °C and 180 °C

indicated in Table 1 shows the formation of more decay product as a consequence of ageing at a higher temperature.

### 3.4.2 FTIR analysis

Figure 13 shows the FTIR spectra obtained for virgin oil and thermally aged oil samples. Elevated temperature acts as a catalyst for oxidative degradation. With ageing more acid and carbonyl compounds are formed in the oil. Ester oil exhibits a broad fingerprint changes in 600–1700  $\text{cm}^{-1}$  range. It is difficult to identify fingerprint peaks due to overlapping regions corresponding to C–O, C–N, C=N, C–C and C=C bonds. The stretching of the C–O–C fingerprint region corresponds to the impact of thermal oxidative reactions.

### 3.4.3 Dynamic viscosity

The presence of triple unsaturated fatty acids with low oxidation stability results in low initial viscosity in the virgin sample [34]. Though thermal ageing in ester is reportedly free of sludge formation, a slight increase in viscosity is observed as the oil ages particularly at higher temperatures due to the oxidative breakdown of unsaturated bonds. The

viscosity values for oil were calculated at 30 °C at a shear rate of  $100 \text{ s}^{-1}$  (Table 1).

### 3.4.4 Turbidity

Table 1 shows the value for turbidity of thermally aged oil samples. Increase in turbidity is observed with thermal ageing at higher temperatures and is attributed to an increase in decay products formed due to ageing. Hjadad et al. have proposed the assessment of the ageing status of oil using UV and turbidity measurement as they offer a reliable and quick assessment. A close correlation between turbidity and DDP exists which can help trace impurities in oil [35].

### 3.4.5 Thermal conductivity

As oil insulation is also expected to provide cooling inside the transformer tank, its ability of heat conduction is of prime importance. Table 1 shows a marginal decrease in the thermal conductivity value of oil aged at a higher temperature. Enhanced viscosity hinders the motion of fluid by increasing inter-layer friction, which can degrade the heat conduction capacity of oil. Viertel et al. have reported that degradation of ester oil primarily begins with decomposition of antioxidants followed by oxidative reaction of the non-oleic fatty acid components with respect to ageing temperature. This is a long-run mechanism, which depends upon the oleic acid content in the triglyceride structure of ester [36].

### 3.4.6 Moisture content

Moisture ingress in oil as a consequence of ageing greatly accelerates the hydrolytic breakdown of hydrocarbon bonds. The temperature of ageing greatly influences the equilibrium moisture distribution. As seen in Table 1, oil aged at 180 °C (Sample C) has the highest moisture content. Enhanced moisture content affects the polarization and depolarization process, enhancing its permittivity and dielectric loss (Figs. 10, 11). Reports indicate natural ester oils show

high dielectric breakdown strength for moisture content up to 350 ppm. In the current analysis, ageing at 140 °C and above shows considerably higher moisture content which can explain the reduction in CIV values (Fig. 3). Liao et al. [37] have reported enhanced acid content and relative moisture in ester oil due to ageing leads to a reduction in dielectric strength.

## 4 Conclusions

The present study provides interesting insights into the thermal ageing mechanism by analysing the impact of ageing on ionic properties in the oil. The major conclusions arrived at based on the present study are the following:

- Thermal ageing of natural ester oil at higher temperature reduces the corona inception voltage.
- The UHF signal formed due to corona activity in ester oil shows dominant frequency at near 1 GHz and the energy content lies in the range of 0.4–4 GHz. The UHF signal magnitude formed and its energy content has a direct correlation. The magnitude of the UHF signal formed is high with thermally aged specimen carried out at higher temperatures.
- Time of flight of polarization current is observed to decrease as the applied voltage increases due to the electrohydrodynamic effect. The peak current value is observed to increase with the increase in applied voltage.
- Ionic mobility is observed to increase with thermally aged specimens. This is accompanied by an increase in concentration and conductivity of oil samples with ageing. Due to thermal degradation, the average ionic radii decrease with ageing which could be due to the hydrolytic breakdown of triglyceride ester bonds.
- Permittivity value increases with an increase in thermal ageing temperature, which leads to enhanced loss. The dissipation factor of oil, aged at a higher temperature, shows higher value, which indicates a negative impact of thermal ageing temperature.
- Physicochemical changes in oil occur due to ageing which leads to a redshift in UV spectra. The area under the absorbance curve associated with Dissolved Decay Product is observed to increase with ageing.
- FTIR analysis of oil exhibits an increment in transmittance in 600–1700  $\text{cm}^{-1}$  region. The region corresponds to overlapping peaks of C–O, C–N, C=N, C–C and C=C bonds.
- Thermal ageing at higher temperature leads to a proportional increase in viscosity and turbidity of oil. This hampers the heat conduction of oil, as indicated by the reduced thermal conductivity values for aged oil sample.

- An increase in moisture content in the oil is observed with thermal ageing carried at high temperature. This leads to enhanced polarization and depolarization current, which can explain the increases in the ionic mobility of oil samples aged at elevated temperatures.

## References

1. Martin D, Saha T, McPherson L (2017) Condition monitoring of vegetable oil insulation in in-service power transformers: some data spanning 10 years. *IEEE Electr Insul Mag* 33(2):44–51
2. Fofana I, Bouaïcha A, Farzaneh M, Sabau J, Bussièrès D, Robertson EB (2010) Decay products in the liquid insulation of power transformers. *IET Electr Power Appl* 4(3):177–184
3. Muhamad NA, Phung BT, Blackburn TR (2012) Application of common transformers faults diagnosis methods on biodegradable oil-filled transformers. *Electr Eng* 94(4):207–216
4. Balasubramanian M, Ravi G, Dharmalingam V (2012) Interdependence of thermal and electrical stresses on initiating degradation of transformer insulation performances. In: *IEEE international conference on advances in engineering, science and management (ICAESM-2)*, pp 399–402
5. Jabloski M, Juszczak EN (2006) Internal faults in power transformers. *IET Electr Power Appl* 1(1):105–111
6. Park TW, Han SH (2017) Numerical analysis of local hot-spot temperatures in transformer windings by using alternative dielectric fluids. *Electr Eng* 97(4):261–268
7. Radakovic Z, Maksimovic S (2002) Non-stationary thermal model of indoor transformer stations. *Electr Eng* 84(2):109–117
8. Bandara K, Ekanayake C, Saha T, Ma H (2016) Performance of natural ester as a transformer oil in moisture-rich environments. *Energies* 9(4):258–271
9. Judd MD, Cleary GP, Bennoch CJ (2002) Applying UHF partial discharge detection to power transformers. *IEEE Power Eng Rev* 22(8):57–59
10. Islam MM, Lee G, Hettiwatte SN (2018) A review of condition monitoring techniques and diagnostic tests for lifetime estimation of power transformers. *Electr Eng* 100(2):581–605
11. Stringer AD, Thompson CC, Barriga CI (2019) Analysis of historical transformer failure and maintenance data for facility reliability. In: *Conference record—industrial and commercial power systems technical conference*, vol 2019
12. Bartnikas R (1967) Dielectric loss in insulating liquids. *IEEE Trans Electr Insul* 2(1):33–54
13. Wang SQ, Zhang GJ, Wei JL, Yang SS, Dong M, Huang XB (2010) Investigation on dielectric response characteristics of thermally aged insulating pressboard in vacuum and oil-impregnated ambient. *IEEE Trans Dielectr Electr Insul* 17(6):1853–1862
14. Yang L, Zadeh MS, Schiessling J, Hjortstam O, Serdyuk YV, Gubanski SM (2012) Measurement of ion mobility in transformer oils for HVDC applications. In: *ICHVE 2012–2012 international conference on high voltage engineering and application*, pp 464–467
15. Lv Y, Du Q, Wang L, Sun Q, Huang M, Li C, Qi B (2017) Effect of TiO<sub>2</sub> nanoparticles on the ion mobilities in transformer oil-based nanofluid. *AIP Adv* 7(10):105022
16. Yang L, Gubanski S, Serdyuk YV, Schiessling J (2012) Dielectric properties of transformer oils for HVDC applications. *IEEE Trans Dielectr Electr Insul* 19(6):1926–1933
17. IEEE Std C57.147™ (2008) IEEE Std C57.147™-2011-guide for acceptance and maintenance of natural ester fluids in transformers

18. IEC 60247 (2004) Insulating liquids—measurement of relative permittivity, dielectric dissipation factor ( $\tan \delta$ ) and d.c. resistivity
19. Azcarraga CG, Cavallini A, Piovani U (2014) A comparison of the voltage withstand properties of ester and mineral oils. *IEEE Electr Insul Mag* 30(5):6–14
20. Xiang J, Liu Q, Wang ZD (2016) Inception and breakdown voltages of insulating liquids under DC stress. In: ICHVE 2016—2016 IEEE international conference on high voltage engineering and application, pp 1–4
21. Beroual A, Zahn M, Badent A, Kist K, Schwabe AJ, Yamashita H, Yamazawa K, Danikas M, Chadband WD, Torshin Y (1998) Propagation and structure of streamers in liquid dielectrics. *IEEE Electr Insul Mag* 14(2):6–17
22. Devins JC, Rzad SJ, Schwabe RJ (1981) Breakdown and prebreakdown phenomena in liquids. *J Appl Phys* 52(7):4531–4545
23. Judd MD, Cleary GP (2006) UHF and current pulse measurements of partial discharge activity in mineral oil. *IEE Proc Sci Meas Technol* 153(2):47–54
24. Adamczewski I, Januszajtis A (1996) Progress in understanding of ionization conduction and breakdown in dielectric liquids. In: ICDL'96. 12th international conference on conduction and breakdown in dielectric liquids, pp 148–151
25. Watanabe M, Sanui K, Ogata N, Kobayashi T, Ohtaki Z (1985) Ionic conductivity and mobility in network polymers from poly(propylene oxide) containing lithium perchlorate. *J Appl Phys* 57(1):123–128
26. IEC 61620 (1998) Insulating liquids—determination of the dielectric dissipation factor by measurement of the conductance and capacitance—test method
27. Onsager L (1934) Deviations from Ohm's law in weak electrolytes. *J Chem Phys* 2(9):599–615
28. Choe E, Min DB (2007) Chemistry of deep-fat frying oils. *J Food Sci* 72(5):77–86
29. André D (2011) Conduction and breakdown initiation in dielectric liquids. In: Proceedings—IEEE international conference on dielectric liquids, pp 1–11
30. Singha S, Asano R, Frimpong G, Claiborne C, Cherry D (2014) Comparative aging characteristics between a high oleic natural ester dielectric liquid and mineral oil. *IEEE Trans Dielectr Electr Insul* 21(1):149–158
31. Jonscher AK (1996) Universal relaxation law, 2nd edn. Chelsea Dielectric Press Limited, London
32. Saha TK, Darveniza M, Yao ZT, Hill DJT, Yeung G (1999) Investigating the effects of oxidation and thermal degradation on electrical and chemical properties of power transformers insulation. *IEEE Trans Power Deliv* 14(4):1359–1367
33. ASTM-6802 (2010) Test method for determination of the relative content of dissolved decay products in mineral insulating oils by spectrophotometry. *ASTM Designation D 6802 Vol 10.03*
34. Fernández I, Ortiz A, Delgado F, Renedo C, Pérez S (2013) Comparative evaluation of alternative fluids for power transformers. *Electr Power Syst Res* 98:58–69
35. Hadjadj Y, Fofana I, Sabau J, Brioso E (2015) Assessing insulating oil degradation by means of turbidity and UV/VIS spectrophotometry measurements. *IEEE Trans Dielectr Electr Insul* 22(5):2653–2660
36. Viertel J, Ohlsson K, Singha S (2011) Thermal aging and degradation of thin films of natural ester dielectric liquids. In: Proceedings—IEEE international conference on dielectric liquids, pp 1–4
37. Liao R, Hao J, Chen G, Ma Z, Yang L (2011) A comparative study of physicochemical, dielectric and thermal properties of pressboard insulation impregnated with natural ester and mineral oil. *IEEE Trans Dielectr Electr Insul* 18(5):1626–1637

**Publisher's Note** Springer Nature remains neutral with regard to jurisdictional claims in published maps and institutional affiliations.